Research Article – Vol. 02, Issue 02, No. 04

Advanced in Engineering and Intelligence Systems

Journal Web Page: https://aeis.bilijipub.com

Size-Dependent Dynamic Behavior of Axially Moving Graphene Nanosheets using Nonlocal First-Order Shear Deformation Theory

Huafeng Tian[1,*]

[1] *Beijing Technology and Business University, Fangshan District, China, 102401*

Highlights

- Investigation of vibration behavior of graphene nanosheets under axial motion for sensor design.
- Modified couple stress theory and Kirchhoff's nonlinear plate model used to analyze nanosheet behavior.
- Hamilton's principle employed to derive nonlinear equations, solved using Galerkin method.
- Small size parameter increases critical speed and oscillation frequency of nanosheet system.
- Study concludes that nanosheet motion exhibits chaotic instability, relevant for nanostructure applications.

Article Info

Received: 14 February 2023
Received in revised: 10 April 2023
Accepted: 10 April 2023
Available online: 29 June 2023

Keywords

Vibrations,
Graphene nanosheets,
Axial motion,
Modified coupling stress,
natural frequency.

Abstract

Based on the potential applications of graphene nanosheets as super-sensitive sensors, this paper examines the vibrations of graphene nanoplates under the influence of axial motion. For this purpose, Kirchhoff's nonlinear plate model will be used in conjunction with the modified couple stress theory (MCST). Using Hamilton's principle, nonlinear equations governing motion are extracted and then discretized using the Galerkin method. Based on the numerical method, the dynamic response and vibration characteristics of these systems are determined. According to our results, the small size parameter increases the critical speed of the system. The first non-dimensional critical speed of the system at 0, 1.2, and 1.8 is approximately 3.14, 3.18, and 3.42, respectively. A small size parameter also increases the system's oscillation frequency. It is unnecessary to apply the modified stress coupling theory to nanosheets with thicker thicknesses ($h > 1.25l$) since the effect of the size scale parameter increases with decreasing thickness. In contrast, the frequency increases significantly for thinner nanosheets. Due to the nonlinear behavior of these systems, the instability of the motion of the system can be attributed to chaotic behavior based on the study of the dynamic response. Graphene nanosheets and other plate-like nanostructures may be identified based on the results presented here.

1. Introduction

Recent advances in nanotechnology and the widespread use of structures with small dimensions in engineering applications, particularly in the field of mechanical and electrical engineering have led to an increased interest in analyzing and understanding the behavior of microstructures. The use of nanostructures in measurement systems as sensors is one of the most important applications of nanostructures. Additionally, these structures can be used to accurately measure the dynamic properties of axially moving systems. Systems of this type may be subject to a variety of phenomena, including resonance, static instability, flutter instability, and maximum vibration amplitudes depending on the axial velocity. As a result, mathematical modeling of these systems is very important to determine their dynamic behavior.

As a result of the fact that classical theories cannot accurately calculate the vibration behavior of nanostructures, nanostructures behavior must be studied

* Corresponding Author: Huafeng Tian
Email: tianhuafeng@st.btbu.edu.cn

using these non-classical theories. The non-local theory [1], strain theory [2], CST [3], and MCST [4] are common and applied non-classical theories. Shaat et al. [5] suggested a size-dependent model based on non-local MCST. Wang et al. [6] examined the simultaneous effects of electrical fields and small dimensions on the stretching instability of rectangular nanosheets regardless of geometric nonlinearities. It was found that the couple stress components did not affect the shape of the nanosheet modes in any way. Couple stress theory has been widely used to analyze the behavior of nanostructures. By the modified couple-stress theory (MCST), Murmu and Shafiei et al. [7] considered the vibration response of single and multilayered graphene sheets. They discovered the classical plate theory frequency is significantly higher than the nonlocal theory frequency for nanoplates. A nonlocal continuum plate model based on single-layered graphene sheets for free vibration analysis was proposed by Zhang et al. [8]. According to the classical plate theory, the molecular dynamic simulations and the nonlocal model for each boundary condition are consistent. The effect of the scale parameter on the buckling of quadrilateral nanoplates has been studied by Ajri et al. [9]. Kiani [10] used nonlocal continuum theory to study the scale parameter of moving nanoparticles subject to Coulomb friction on thin nanoplates. Dynamic responses were investigated based on small-scale parameters, the velocity of moving nanoparticles, and dynamic amplitude factors (DAF) of the transverse and in-plane displacements. An analysis of nanomechanical sensor vibration was carried out by Shen et al. [11] using a nonlocal plate theory that incorporates size effects. Their model allows a nanoparticle with a concentrated micromass to be placed anywhere on a rectangular nanoplate. According to the study, the results tend to be consistent with the classical model without the nonlocal parameter. Thai et al. [12] conducted a static analysis of micro/nanoscale plates using a mesh-free model. They also applied various boundary conditions utilizing the penalty method.

With the propagator matrix method, Guo et al. [13] developed 3D analytical answers to investigated the vibrations of a multilayered composite simply supported nanoplate. According to Shahraki et al. [14], vibration characteristics of nth order rectangular nanoplates are studied using modified couple stress theory. Lin [15] examined the instability and vibration behavior of axially moving plates and expected the instability speed by the linear plate theory. A vibration analysis of axially moving functionally graded nanoplates in a hygrothermal environment has been presented by Zhu et al. [16]. A theoretical description of the nanoplate is provided using Kirchhoff plate theory and the concept of a physical neutral layer. In a recent study, Esmaeilzadeh and Kadkhodayan [17] examined the vibrations of axially moving sandwich nanoplates reinforced with graphene platelets. The results demonstrate that nonlocality and strain gradient parameters play a greater role in dynamic deflections as the nanoplate velocity increases.

There has been some research on axially moving graphene nanosheets using nonlocal first-order shear deformation theory, but there has been no work on free dynamic and instability analysis. Based on the authors' knowledge, the authors present for the first time a dynamic analysis of axially moving graphene nanosheets. Accordingly, the nonlinear equations governing motion are derived utilizing the modified couple stress theory and Kirchhoff's nonlinear plate model. The equations are discretized using Galerkin methods. The dynamic response and vibration characteristics of these systems are determined through the simultaneous numerical solution of these equations.

2. Extraction of motion equations

Figure 1 illustrates a schematic of an axially moving graphene nanosheets. The graphene nanosheets is assumed to move in the longitudinal direction with a constant axial velocity at the boundary conditions of simple abutments. The length, cross-sectional area, and moment of inertia are represented by L, A, and I, respectively. In addition, the thickness of the sheet is also equal to h.

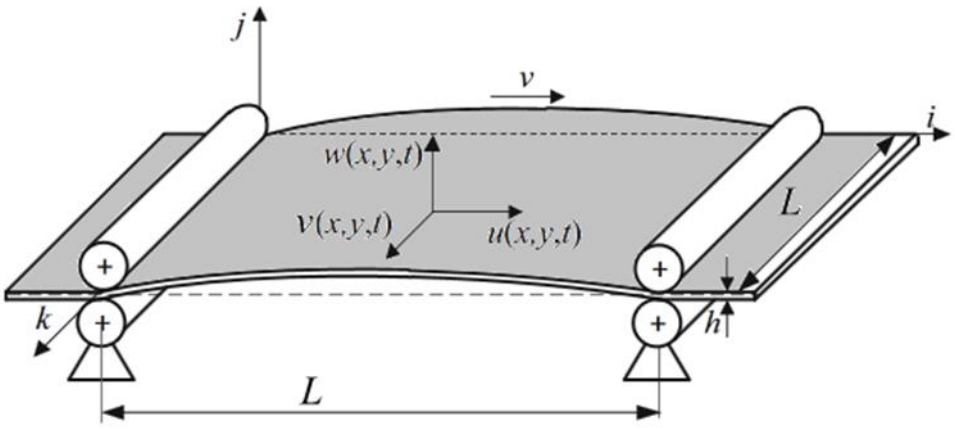

Fig. 1. Axially moving graphene nanosheets with simply supported boundary condition

Modified couple stress theory also includes symmetric curvature tensor in strain energy along with strain tensor. Hence, in the small deformation of linear elastic material, the strain energy is obtained as follows [14]:

$$U = \int \frac{1}{2}\left[\sigma_{ij}\varepsilon_{ij} : m_{ij}\chi_{ij}\right]dV \tag{1}$$

$$\sigma_{ij} = \lambda\varepsilon_{ij} + 2\mu\varepsilon_{ij} \tag{2}$$

$$\varepsilon_{ij} = \frac{1}{2}\left(u_{i,j} + u_{j,i}\right) \tag{3}$$

$$m_{ij} = 2\mu\ell^2\chi_{ij} \tag{4}$$

$$\chi_{ij} = \frac{1}{2}\left(\theta_{i,j} + \theta_{j,i}\right) \tag{5}$$

in which u is the displacement vector, θ is the rotation vector, and ℓ is the scale parameter. Also, λ and μ are the Lame's constants. It should be noted that the relationship between the components of the rotation vector θ and the components of the displacement vector u is as follows:

$$\theta_i = \frac{1}{2}e_{ijk}u_{k,j} \tag{6}$$

According to Kirchhoff's theory of plates, the displacement field of an arbitrary point of the nanosheet in the Cartesian coordinate system is as follows:

$$\begin{aligned} u_1(x,y,z,t) &= -zw_{,x}(x,y,t) + u(x,y,t) \\ u_2(x,y,z,t) &= -zw_{,y}(x,y,t) + v(x,y,t) \\ u_3(x,y,z,t) &= w(x,y,t) \end{aligned} \tag{7}$$

where (u, v, w) represents the displacement field components of an arbitrary point located on the middle surface of the nanosplate, respectively in the x-, y-, and z-directions. Considering the large geometric deformations, the strain-displacement relationship according to von Kármán theory is as follows:

$$\begin{Bmatrix} \varepsilon_x \\ \varepsilon_y \\ \gamma_{xy} \end{Bmatrix} = \begin{Bmatrix} u_{,x} + 0.5w_{,x}^2 \\ v_{,y} + 0.5w_{,y}^2 \\ u_{,y} + u_{,x} + w_{,x}w_{,y} \end{Bmatrix} - z\begin{Bmatrix} w_{,xx} \\ w_{,yy} \\ 2w_{,xy} \end{Bmatrix} \tag{8}$$

Also, the non-zero components of the curvature tensor are obtained based on Eq. (5) as follows:

$$\begin{Bmatrix} \chi_x \\ \chi_y \\ \chi_{xy} \\ \chi_{xz} \\ \chi_{yz} \end{Bmatrix} = \begin{Bmatrix} w_{,xy} \\ -w_{,xy} \\ -\frac{1}{2}\left(w_{,xx} - w_{,yy}\right) \\ -\frac{1}{4}\left(u_{,xy} - v_{,xx}\right) \\ -\frac{1}{4}\left(u_{,yy} - v_{,xy}\right) \end{Bmatrix} \tag{9}$$

To develop the motion equations, we use the Hamilton principle. Based on this principle we will have:

$$\delta\int_0^t (U + T - W_{ext})dt = 0 \tag{10}$$

where U is the strain energy, T stands kinetic energy and W_{ext} stands the work done by external forces.

Based on the MCST, the strain energy of thin nanosheet is calculated as follows:

$$U = \frac{1}{2}\int \begin{pmatrix} \sigma_{xx}\varepsilon_{xx} + \tau_{xy}\gamma_{xy} + \sigma_{yy}\varepsilon_{yy} + m_{xx}\chi_{xx} \\ +2m_{xz}\chi_{xz} + 2m_{xy}\chi_{xy} + 2m_{yz}\chi_{yz} \end{pmatrix} dV \tag{11}$$

where σ is the etress tensore, ε stands the strain components, m and χ remain the nanoscale paramaters.

To compute the kinetic energy, it is necessary to determine the absolute velocity of any desired point of the nanosheet. When the nanosheet is exposed to transverse vibrations, the total displacement vector of each nanosheet point in the Cartesian coordinates (x, y, z) is as:

$$\boldsymbol{r} = (x + u_1)\boldsymbol{i} + (y + v_1)\boldsymbol{j} + (z + w_1)\boldsymbol{k} \tag{12}$$

Therefore, the absolute velocity of the axial moving nanosheet can be obtained by time deriving of Eq. (12) as follows:

$$\boldsymbol{V} = \left[V_0 + \frac{du}{dt} - z\frac{d}{dt}\left(\frac{\partial w}{\partial x}\right)\right]\boldsymbol{i} + \left[\frac{dv}{dt} - z\frac{d}{dt}\left(\frac{\partial w}{\partial y}\right)\right]\boldsymbol{j} + \frac{dw}{dt}\boldsymbol{k} \tag{13}$$

where $\frac{d}{dt} = V_0\frac{\partial}{\partial x} + \frac{\partial}{\partial t}$. As a result, the kinetic energy T of the axial moving nanosheet can be determined as follows:

$$T = \frac{1}{2}\int_V \rho V^2 dV = \frac{\rho h}{2}\int_A \left[\left(V_0 + \frac{du}{dt}\right)^2 + \left(\frac{dv}{dt}\right)^2 + \left(\frac{dw}{dt}\right)^2\right] dA + \frac{\rho h^3}{24}\int_A \left[\left(\frac{d}{dt}\left(\frac{\partial w}{\partial x}\right)\right)^2 + \left(\frac{d}{dt}\left(\frac{\partial w}{\partial y}\right)\right)^2\right] dA \tag{14}$$

where ρ is the density of the nanosheet.

Substituting Eqs. (11) and (14) in Eq. (10) and using strain-displacement Eqs. (8) and (9), the equations governing the transverse vibration behavior of axial moving nanosheet are obtained as follows:

$$N_{x,x} + N_{xy,y} + \frac{1}{2}\left(\Upsilon_{xz,xy} + \Upsilon_{yz,yy}\right) = \rho h\left(\frac{\partial^2 u}{\partial t^2} + 2V_0\frac{\partial^2 u}{\partial x \partial t} + V_0^2\frac{\partial^2 u}{\partial x^2}\right) \tag{15}$$

$$N_{xy,x} + N_{y,y} + \frac{1}{2}\left(\Upsilon_{yz,xy} + \Upsilon_{xz,xx}\right) = \rho h\left(\frac{\partial^2 v}{\partial t^2} + 2V_0\frac{\partial^2 v}{\partial x \partial t} + V_0^2\frac{\partial^2 v}{\partial x^2}\right) \tag{16}$$

$$\left(N_{xy}w_{,x} + N_y w_{,y}\right)_{,y} + \left(N_x w_{,x} + N_{xy}w_{,y}\right)_{,x} + M_{xx,x} + 2M_{xy,xy} + \Upsilon_{yz,xx} - \Upsilon_{xy,yy} + M_{y,yy} + \Upsilon_{y,xy} - \Upsilon_{x,xy} = \rho h\left(\frac{\partial^2 w}{\partial t^2} + 2V_0\frac{\partial^2 w}{\partial x \partial t} + V_0^2\frac{\partial^2 w}{\partial x^2}\right) + \frac{\rho h^3}{12}\left(\frac{\partial^2}{\partial t^2} + 2V_0\frac{\partial^2}{\partial x \partial t} + V_0^2\frac{\partial^2}{\partial x^2}\right)(\nabla^2 w) \tag{17}$$

where N_{ij}, M_{ij} and Υ_{ij} are obtained from the following relations:

$$\{N_x, N_y, N_{xy}\} = \int_{-h/2}^{h/2}\{\sigma_x, \sigma_y, \sigma_{xy}\}dz \tag{18}$$

$$\{M_x, M_y, M_{xy}\} = \int_{-h/2}^{h/2}\{\sigma_x, \sigma_y, \sigma_{xy}\}z dz \tag{19}$$

$$\{\Upsilon_x, \Upsilon_y, \Upsilon_{xy}, \Upsilon_{xz}, \Upsilon_{yz}\} = \mu\ell^2\int_{-h/2}^{h/2}\{\chi_x, \chi_y, \chi_{xy}, \chi_{xz}, \chi_{yz}\}dz \tag{20}$$

Substituting the strain-displacement equations (8) and (9) in the equations (18)-(20), the internal forces and torques are achieved in terms of displacement fields. By substituting the obtained relations in equations (15)-(17), the motion equations are obtained in terms of unknown variables (u, v, w). For the purpose of solving nonlinear differential equations of the coupling governing motion, Galerkin technique is used. Considering the boundary conditions of moving simply supports, the following functions are considered for displacement fields [18]:

$$u(x, y, t) = \sum_{m=1}^{M}\sum_{n=1}^{N} U_{m,n}(t)\, sin\left(\frac{n\pi y}{b}\right) cos\left(\frac{m\pi x}{a}\right) \tag{21}$$

$$v(x, y, t) = \sum_{m=1}^{M}\sum_{n=1}^{N} cos\left(\frac{n\pi y}{b}\right) sin\left(\frac{m\pi x}{a}\right) V_{m,n}(t) \tag{22}$$

$$w(x, y, t) = \sum_{m=1}^{M}\sum_{n=1}^{N} sin\left(\frac{n\pi y}{b}\right) sin\left(\frac{m\pi x}{a}\right) W_{m,n}(t) \tag{23}$$

where $V_{m,n}(t)$, $U_{m,n}(t)$ and $W_{m,n}(t)$ functions are unknown. In order to calculate these unknown functions, Galerkin technique is used. Accordingly, by placing the hypothetical answers (21)-(23) in Eqs. (15)-(17) and applying the Galerkin technique, the nonlinear equations with partial derivatives become nonlinear equations with the following partial derivatives.

$$M\ddot{q} + C\dot{q} + K_{lin}q + K_{non}q^3 = 0 \tag{24}$$

3. Stability analysis

The obtained second-order Eq. (24) can be reduced to first-order equations as:

$$BZ(t) + EZ(t) = 0 \tag{25}$$

where

$$B = \begin{bmatrix} 0 & M \\ M & C \end{bmatrix}, E = \begin{bmatrix} -M & 0 \\ 0 & K \end{bmatrix}, Z = \begin{bmatrix} q \\ \dot{q} \end{bmatrix} \tag{26}$$

Assuming $Z(t) = Ae^{i\omega t}$ we can write:

$$YA - iwI = 0 \qquad (27)$$

in which ***I***is the unit matrix, and $Y = -B^{-1}E$. Additionally, ω is the natural complex frequency of the system, which can be determined by a key system parameter. In frequency, the real and imaginary parts represent the vibrational frequency and damping coefficient, respectively. As a result, the stability of the moving system depends on the sign of the real part of each natural frequency. Divergence instability occurs when at least one of the natural frequency branches has zero real parts, while the imaginary part is negative and the real part is zero. In the divergence event, the speed at which the divergence occurs is known as the critical speed. The Hopf branch experiences flutter instability when at least one of the frequency branches has a negative imaginary part and a positive real part [19-22].

4. Results and Disruptions

The proposed method is first tested for convergence in this section. In addition, the results for the isotropy nanoplate are obtained and compared with those existing in the technical literature. Furthermore, the influence of axial velocity, small size parameters, and large deformation are examined separately and simultaneously, with respect to natural frequencies, dynamic response, and stability limits of axially moving nanosheet. There is also the possibility of calculating the dynamic response of the system numerically using the fourth-order Runge-Kutta method. The presented results are in terms of the following dimensionless parameters:

$$\eta = \sqrt{\frac{\rho h}{D}} LV, \Omega = \omega \sqrt{\frac{D}{\rho h L^4}}, \lambda = \left(\frac{\ell}{h}\right)^2$$

where η, Ω andλ represent the dimensionless velocity, dimensionless natural frequency and dimensionless size parameter, respectively. The geometric and mechanical properties of graphene nanosheet are as: a= 5000 nm, b=5000 nm, h= 0.335 nm, υ=0.36, E=1.02 TPa, and ρ=2300 kg/m^3 [23, 24].

To evaluate the accuracy and convergence of the results, the number of sentences within the Galerkin method must first be considered. According to the Galerkin method, Figure 2 shows the changes in axial velocity associated with the first three natural frequencies per different number of sentences. Results demonstrate that the first two forms of the mode for 5 Galerkin sentences converge and that the results for 5 sentences and 10 sentences are not significantly different. Since the shape of the third mode tends to converge after ten sentences, the results are derived in this investigation after ten sentences.

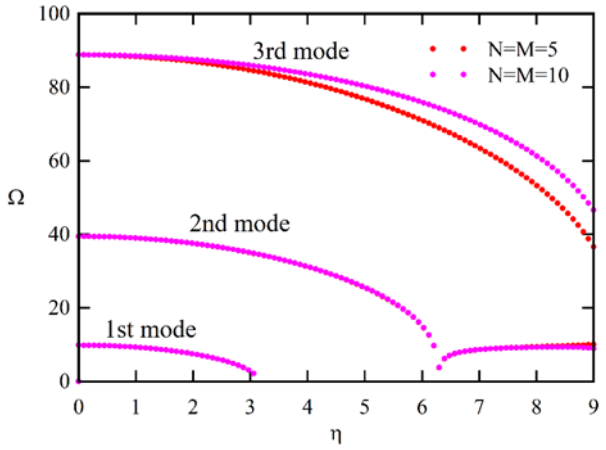

Fig. 2 Effect of the number of sentences in the Galerkin method on the convergence of results

4.1.Validation of results

In view of the fact that the behavior of nonlinear vibrations of graphene nanosheets under axial motion has not yet been investigated, the linear behavior is validated. Ignoring the effects of nonlinear sentences, Figure 3 shows the real part of the three dimensionless natural frequencies of the axially moving nanosheet. The results achieved from the present work are dependable with those obtained by Arani et al. [25]. There is a discrepancy between the critical velocities of the present study and the reference results [25] as a result of the difference between the theories employed. According to Figure 3, it can be demonstrated that the maximum critical axial speed error of the current research is around 3%.

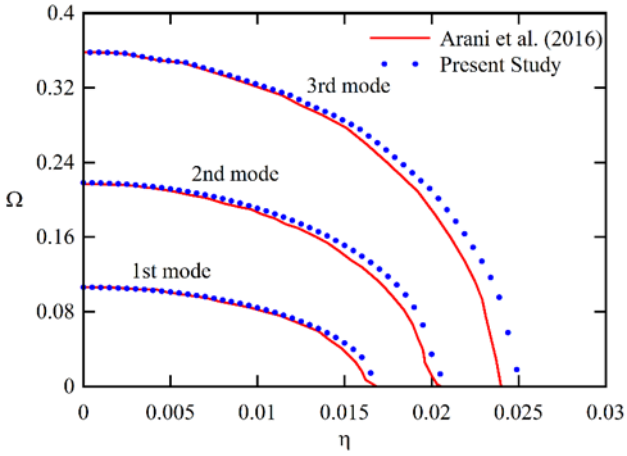

Fig. 3 An analysis of the relationship between dimensionless frequency and dimensionless axially moving speed for first three vibration modes.

4.2. Effect of the small size parameter

The curves of the imaginary and the real parts of the first three natural frequencies of nanoplate are depicted in Figures 4a and 4b, respectively, according to the speed of

the moving nanofilter and for varying values of the small size parameter. Interestingly, when the velocity of the foil is zero, its natural frequencies are purely imaginary. With increasing speed, the imaginary part of the eigenvalues representing the natural frequencies decreases slowly, while the real part remains constant. The imaginary part of the base frequency of the system becomes zero at the critical speed η_{cr}. After this point, the system becomes unstable and buckles. This condition is known as divergence. Further increases in speed lead to the base frequency becoming completely real, while the 2nd frequency decreases uniformly. Further acceleration results in a restoration of stability due to the gyroscopic effect. Therefore, the starting and ending points of the divergence instability are related to the disappearance of the real and imaginary parts of the base frequency, respectively. Finally, the imaginary parts of the 1st and 2nd natural frequencies are combined by a branch of a Paıdoussis-type flutter mode instability, whereas their imaginary parts are divided into two branches with positive and negative values, causing the system to be unstable. In fact, in addition to speeds below the critical speed, there is a narrow speed range in the operating range of the system (between the end of the divergence zone and the beginning of the flutter zone) in which the system is also steady. It should be noted that once the filter passes the critical speed, the system will no longer be stable. This study concludes that the moving nanosheet undergo the process of stable evolution of the stable mode of the first mode divergence of continuity. Another consequence of Figure 4a is that as the small size parameter is increased, the imaginary part of the system frequencies decreases, especially in the higher modes, which demonstrate a more dramatic decline. The result shows that the small size parameter increases the critical speed of the system and for λ at 0, 1.2, and 1.8 the first two-dimensional critical speed is approximately 3.14, 3.18, and 3.42. The explanation for this can be found in the fact that since the small size parameter is a part of the stiffness matrix, any increase in this parameter results in a more stringent system and an extension of the stability zone.

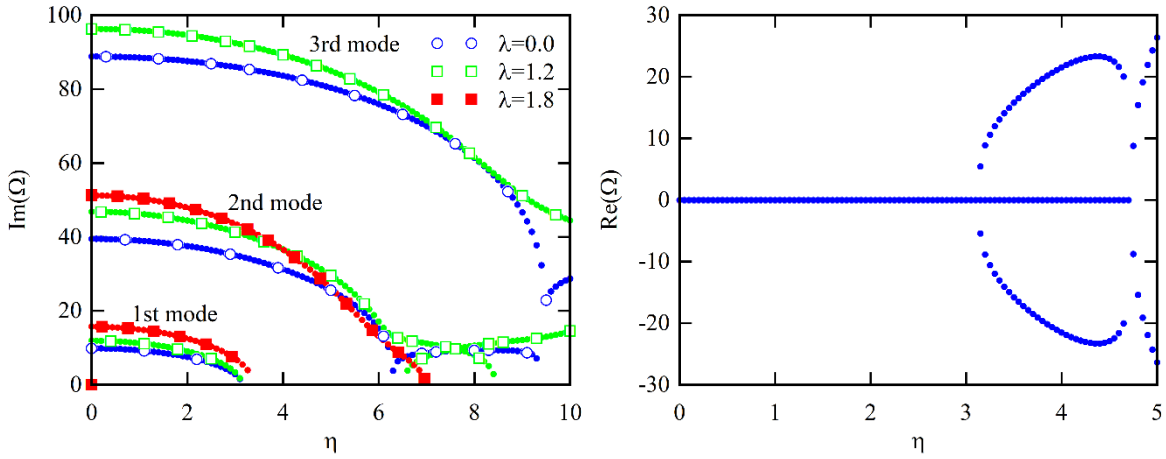

Fig. 4 (a) Real part (b) Imaginary part of the axially moving nanosheet frequencies

In Figure 5, we explore the impact of the size parameter on the first and second critical dimensionless velocities of axial moving nanosheet. As can be seen, increasing the small size parameter increases the critical velocity, and by growing the parameter from 0 to 2, the dimensionless critical velocity increases by approximately 10%.

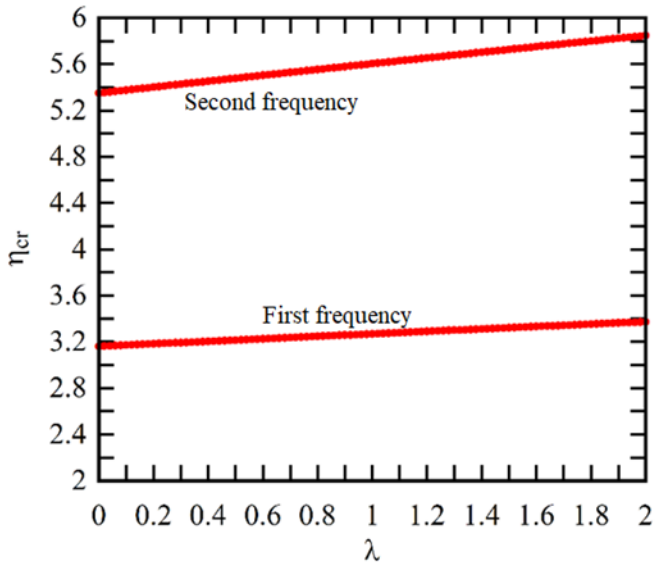

Figure 5 Influence of scale parameter on the first and second dimensional critical velocities of axial moving nanosheet

Figure 6 illustrates the frequencies obtained from the modified stress coupling theory for axially moving nanosheet. We observe that the scale parameter increases the oscillation frequency of the system, and by decreasing the thickness of the nanoplate, the influence of the small size parameter is amplified. It could thus be concluded that for thicker nanosheets ($h > 1.25l$), the MCST is not required, while for thinner nanosheets, the frequency increase is significant.

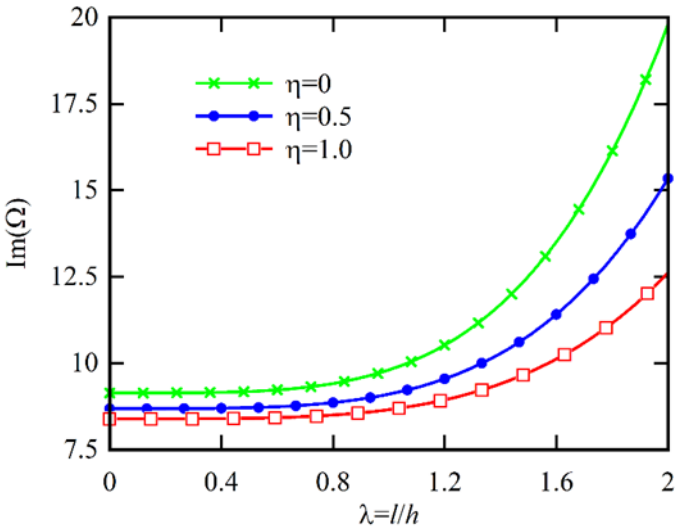

Fig. 6 Influence of scale parameter on the natural first frequency dimension of axial moving nanosheet at different velocities

4.3. Dynamic response

The vibration time response of axially moving nanosheet is studied in this section. Figures 7 through 9 illustrate the influence of axial velocity on the time response of the midpoint of the nanosheet and the phase curve. According to the results, the axial velocity has a significant influence on the vibration response of nanosheet, and as the axial velocity increases, the amplitude of vibrations also increases. In addition, according to Figure 9, the motion of the system around the point of instability is chaotic, which is due to the nonlinear behavior of these systems.

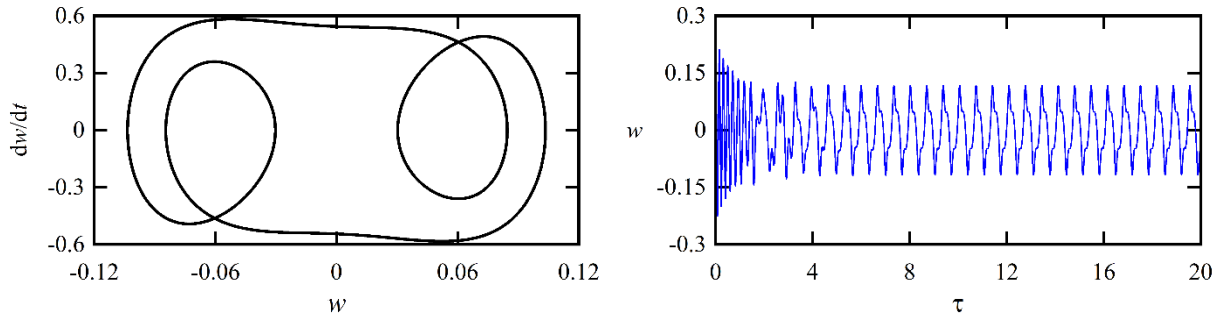

Fig. 7 Time response and phase curve of axial moving nanosheet for $\upsilon = 0.1$

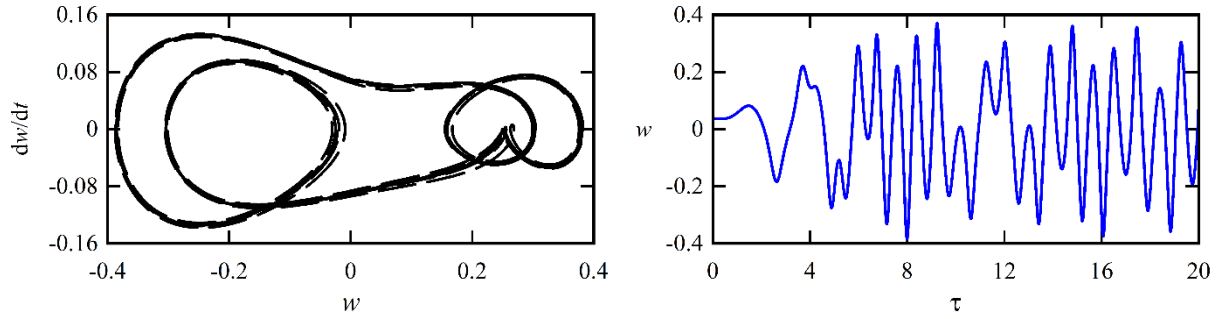

Fig. 8 Time response and phase curve of axial moving nanosheet for $\upsilon = 2$

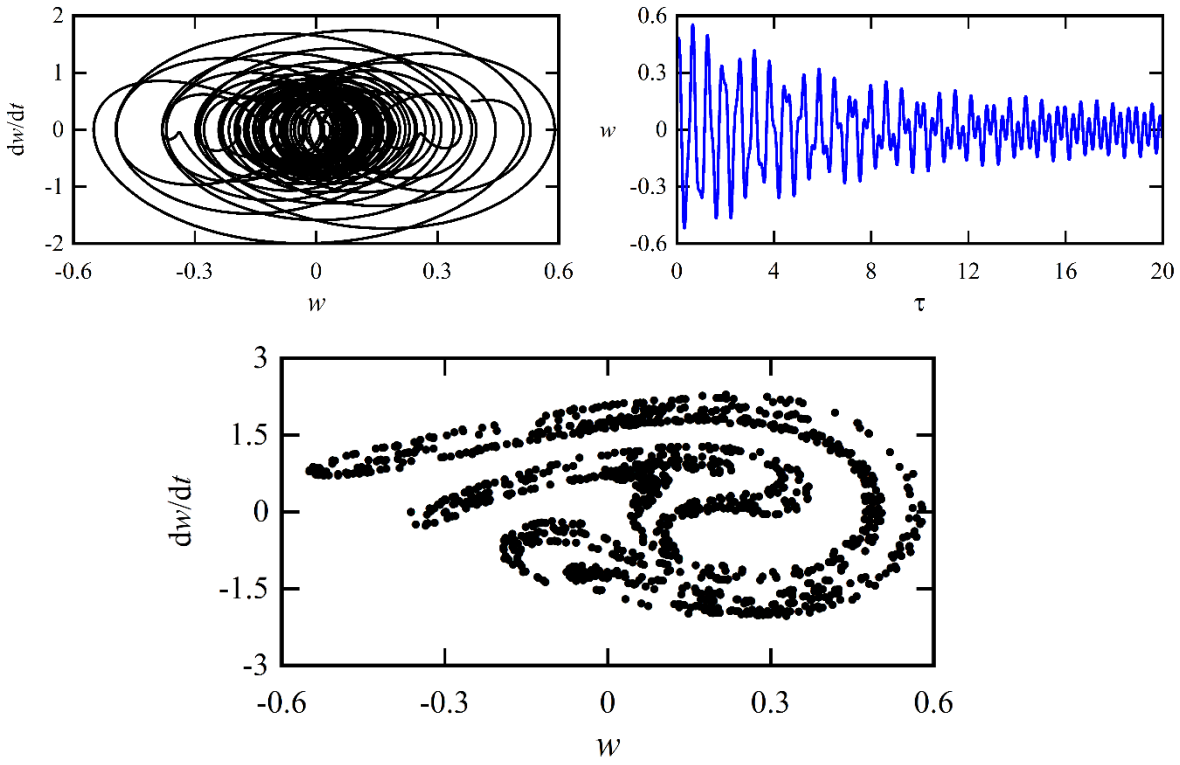

Fig. 9 Time trace and phase curve of axial moving nanosheet for $\upsilon = 3.14$

5. Conclusion

In this study, we investigated the transverse vibration behavior and nonlinear dynamics of graphene nanosheet under axial motion using modified coupling stress theory. To derive the equations of motion, geometric nonlinear effects were taken into account and Hamilton's principle was applied. The natural frequencies and the system

response were derived after discretizing the nonlinear equations that govern the motion using the Galerkin method.

- The vibrating of moving nanoplates was found to be strongly reliant on the speed at which they moved, such that as speed increased, system stability decreased and divergence buckling became more likely to occur.
- The application of nonlinear theory led to a significant increase in the frequency of the nanoplate.
- Scale parameters affect both the divergence instability zero as well as the divergence speed of axially moving nanosheets. Such influences become more substantial when $\lambda > 0.8$. The resultss is hoped to be used in optimum design of modern NEMS/MEMS equipment's in small scale.

REFERENCES

[1] Rezaee, M., Sharafkhani, N. (2019). Nonlinear dynamic analysis of an electrostatically actuated cylindrical micro-beam subjected to cross fluid flow. International Journal of Applied Mechanics, 11(06), 1950061.

[2] Rezaee, M., Sharafkhani, N. (2017). Electrostatically frequency tunable micro-beam-based piezoelectric fluid flow energy harvester. Smart Materials and Structures, 26(7), 075008.

[3] Wu, C.-P., Hu, H.-X., (2021). A unified size-dependent plate theory for static bending and free vibration analyses of micro-and nano-scale plates based on the consistent couple stress theory. Mechanics of Materials. 162 pp. 104085.

[4] Al-Furjan, M., Samimi-Sohrforozani, E., Habibi, M., won Jung, D., Safarpour, H., (2021). Vibrational characteristics of a higher-order laminated composite viscoelastic annular microplate via modified couple stress theory. Composite Structures. 257 pp. 113152.

[5] Shaat, M., Mahmoud, F., Gao, X.-L., Faheem, A. F., (2014). Size-dependent bending analysis of Kirchhoff nano-plates based on a modified couple-stress theory including surface effects. International Journal of Mechanical Sciences. 79 pp. 31-37.

[6] Wang, K., Kitamura, T., Wang, B., (2015). Nonlinear pull-in instability and free vibration of micro/nanoscale plates with surface energy–a modified couple stress theory model. International Journal of Mechanical Sciences. 99 pp. 288-296.

[7] Shafiei, Z., Sarrami-Foroushani, S., Azhari, F., Azhari, M., (2020). Application of modified couple-stress theory to stability and free vibration analysis of single and multi-layered graphene sheets. Aerospace Science and Technology. 98 pp. 105652.

[8] Zhang, Y., Lei, Z., Zhang, L., Liew, K., Yu, J., (2015). Nonlocal continuum model for vibration of single-layered graphene sheets based on the element-free kp-Ritz method. Engineering Analysis with Boundary Elements. 56 pp. 90-97.

[9] Ajri, M., Seyyed Fakhrabadi, M. M., (2018). Nonlinear free vibration of viscoelastic nanoplates based on modified couple stress theory. Journal of Computational Applied Mechanics. 49 (1), pp. 44-53.

[10] Kiani, K., (2011). Small-scale effect on the vibration of thin nanoplates subjected to a moving nanoparticle via nonlocal continuum theory. Journal of Sound and Vibration. 330 (20), pp. 4896-4914.

[11] Shen, Z.-B., Tang, H.-L., Li, D.-K., Tang, G.-J., (2012). Vibration of single-layered graphene sheet-based nanomechanical sensor via nonlocal Kirchhoff plate theory. Computational Materials Science. 61 pp. 200-205.

[12] Thai, C. H., Ferreira, A., Nguyen-Xuan, H., Phung-Van, P., (2021). A size dependent meshfree model for functionally graded plates based on the nonlocal strain gradient theory. Composite Structures. 272 pp. 114169.

[13] Guo, J., Chen, J., Pan, E., (2017). Free vibration of three-dimensional anisotropic layered composite nanoplates based on modified couple-stress theory. Physica E: Low-dimensional Systems and Nanostructures. 87 pp. 98-106.

[14] Eskandari Shahraki, M., Shariati, M., Azarafza, R., Heydari Beni, M., Eskandari Jam, J., (2022). Vibration analysis of an nth order shear deformation nanoplate using the modified couple stress theory. International Journal of Nonlinear Analysis and Applications. pp. -.

[15] Lin, C., (1997). Stability and vibration characteristics of axially moving plates. International Journal of Solids and Structures. 34 (24), pp. 3179-3190.

[16] Zhu, C., Yan, J., Wang, P., Li, C., (2021). A Nonlocal Strain Gradient Approach for Out-of-Plane Vibration of Axially Moving Functionally Graded Nanoplates in a Hygrothermal Environment. Shock and Vibration. 2021 pp.

[17] Esmaeilzadeh, M., Kadkhodayan, M., (2019). Numerical investigation into dynamic behaviors of axially moving functionally graded porous sandwich nanoplates reinforced with graphene platelets. Materials Research Express. 6 (10), pp. 1050b7.

[18] Amabili, M., Nonlinear vibrations and stability of shells and plates. 2008: Cambridge University Press.

[19] Rezaee, M., Arab Maleki, V., (2017). Vibration Characteristics of Fluid-Conveying Pipes in presence of a Dynamic Vibration Absorber.

Modares Mechanical Engineering. 17 (7), pp. 31-38.
[20] Rezaee, M., Maleki, V. A., (2015). An analytical solution for vibration analysis of carbon nanotube conveying viscose fluid embedded in visco-elastic medium. Proceedings of the Institution of Mechanical Engineers, Part C: Journal of Mechanical Engineering Science. 229 (4), pp. 644-650.
[21] Rezaee, M., Arab Maleki, V., (2019). Passive vibration control of fluid conveying pipes using dynamic vibration absorber. Amirkabir Journal of Mechanical Engineering. 51 (3), pp. 111-120.
[22] Pham, P.-T., Hong, K.-S., (2020). Dynamic models of axially moving systems: A review. Nonlinear Dynamics. 100 (1), pp. 315-349.
[23] Pourreza, T., Alijani, A., Maleki, V. A., Kazemi, A., (2021). Nonlinear vibration of nanosheets subjected to electromagnetic fields and electrical current. Advances in nano research. 10 (5), pp. 481-491.
[24] Pourreza, T., Alijani, A., Maleki, V. A., Kazemi, A., (2022). The effect of magnetic field on buckling and nonlinear vibrations of Graphene nanosheets based on nonlocal elasticity theory. International Journal of Nano Dimension. 13 (1), pp. 54-70.
[25] Arani, A. G., Haghparast, E., Zarei, H. B., (2016). Nonlocal vibration of axially moving graphene sheet resting on orthotropic visco-Pasternak foundation under longitudinal magnetic field. Physica B: Condensed Matter. 495 pp. 35-49.